

# CrystEngComm

Accepted Manuscript



This is an *Accepted Manuscript*, which has been through the Royal Society of Chemistry peer review process and has been accepted for publication.

*Accepted Manuscripts* are published online shortly after acceptance, before technical editing, formatting and proof reading. Using this free service, authors can make their results available to the community, in citable form, before we publish the edited article. We will replace this *Accepted Manuscript* with the edited and formatted *Advance Article* as soon as it is available.

You can find more information about *Accepted Manuscripts* in the [Information for Authors](#).

Please note that technical editing may introduce minor changes to the text and/or graphics, which may alter content. The journal's standard [Terms & Conditions](#) and the [Ethical guidelines](#) still apply. In no event shall the Royal Society of Chemistry be held responsible for any errors or omissions in this *Accepted Manuscript* or any consequences arising from the use of any information it contains.

Cite this: DOI: 10.1039/c0xx00000x

www.rsc.org/xxxxxx

ARTICLE TYPE

# Polyoxometalate-directed assembly of various multinuclear metal–organic complexes with 4-amino-1,2,4-triazole and selective photocatalysis for organic dyes degradation †

Xiu-Li Wang\*, Chun-Hua Gong, Ju-Wen Zhang, Guo-Cheng Liu, Xiao-Min Kan, Na Xu

Received (in XXX, XXX) Xth XXXXXXXXX 20XX, Accepted Xth XXXXXXXXX 20XX

DOI: 10.1039/b000000x

A series of polyoxometalate (POM)-based metal–organic complexes containing multinuclear Cu(II) clusters with 4-amino-1,2,4-triazole (4-atrz) ligand, namely,  $[\text{Cu}_3(4\text{-atrz})_8(\text{PMo}_{12}\text{O}_{40})(\text{H}_2\text{O})_2] \cdot 2\text{H}_2\text{O}$  (**1**),  $[\text{Cu}_2(4\text{-atrz})_6(\text{SiW}_{12}\text{O}_{40})(\text{H}_2\text{O})] \cdot 6\text{H}_2\text{O}$  (**2**),  $[\text{Cu}_2(4\text{-atrz})_4(\mu_2\text{-OH})(\text{CrMo}_6(\text{OH})_6\text{O}_{18})] \cdot 3\text{H}_2\text{O}$  (**3**),  $[\text{Cu}_3(4\text{-atrz})_3(\text{Mo}_8\text{O}_{27})(\text{H}_2\text{O})_4] \cdot 6\text{H}_2\text{O}$  (**4**) and  $[\text{Cu}_3(4\text{-atrz})_3(\text{V}_{10}\text{O}_{30})_{0.5}(\mu_3\text{-OH})(\text{H}_2\text{O})] \cdot \text{H}_2\text{O}$  (**5**) have been synthesized by selectively adding additional citric acid or boric acid under hydrothermal conditions and structurally characterized by single-crystal X-ray diffraction and powder X-ray diffraction. Compound **1** is a zero-dimensional (0D) architecture, which is constructed from a linear trinuclear cluster  $[\text{Cu}_3(4\text{-atrz})_8(\text{H}_2\text{O})_2]^{6+}$  and two Keggin  $\text{PMo}_{12}\text{O}_{40}^{3-}$  anions. Compound **2** shows a 1D zigzag chain, in which the binuclear  $[\text{Cu}_2(4\text{-atrz})_6(\text{H}_2\text{O})]^{4+}$  clusters and Keggin  $\text{SiW}_{12}\text{O}_{40}^{4-}$  anions connect each other. Compound **3** is a 1D linear chain based on the linear  $[\text{Cu}_3(4\text{-atrz})_6]^{6+}$  clusters, the  $[\text{CrMo}_6(\text{OH})_6\text{O}_{18}]^{3-}$  anions hang on two sides of the 1D chain. Compound **4** is a 2D layer constructed from trigonal  $[\text{Cu}_3(4\text{-atrz})_3(\text{H}_2\text{O})_4]^{6+}$  clusters and rare infinite  $[\text{Mo}_8\text{O}_{27}]_n^{6n-}$  chains. The  $[\text{Mo}_8\text{O}_{27}]^{6-}$  anion is transformed from the Anderson-type  $[\text{CoMo}_6(\text{OH})_6\text{O}_{18}]^{3-}$  anion, which is also rare in the POM-based reaction system. Compound **5** is a 3D framework constructed from the trigonal trinuclear  $[\text{Cu}_3(4\text{-atrz})_3(\text{OH})]^{5+}$  clusters and rare  $[\text{V}_{10}\text{O}_{30}]^{10-}$  polyanions, which represents the first example of  $\text{V}_{10}\text{O}_{30}$ -based 3D metal–organic complex. Structural analyses indicate that different POMs show great effect on the various structures of **1–5** and the additional acids play an important role in the formation of **1–5**. The photocatalytic experiments of **1–5** on degradation of three organic dyes (methylene blue, rhodamine B and methyl orange) manifest that compounds **1–3** are good candidates for the photocatalytic degradation of methylene blue, and compound **1** is a good photocatalyst for the degradation of rhodamine B.

## Introduction

The design and construction of metal–organic complexes (MOCs) through the organic derivatization of polyoxometalates (POMs) constitutes a current topic within the fields of crystal engineering and material chemistry, not only due to their charming structures, but also due to their versatile application in the fields of photochemistry, clinical chemistry, magnetism, electric device, catalysis and material science.<sup>1</sup> As the well known family of anionic metal-oxygen clusters with large amounts of terminal O atoms ( $\text{O}_t$ ) and bridging O atoms ( $\text{O}_b$ ),

controllable shapes and sizes, high negative charges and various properties,<sup>2</sup> POMs have been comprehensively used as inorganic building blocks to construct novel diverse POMs-based MOCs, which may confer new properties on the resulting hybrid species.<sup>3</sup> Currently, reports on the covalent attachment of multinuclear metal clusters to various polyoxoanions are relatively limited. Thus, how to introduce multinuclear metal clusters into POMs has been one hot subject for researchers.

As is known, organic ligands play a key role in constructing multinuclear metal clusters. The multidentate ligands with more adjacent coordination sites, such as triazole and tetrazole derivatives may aggregate metal ions and conduce to construction of multinuclear clusters. A judicious selection of POMs may yield new materials with fascinating structures and desirable properties. Several types of POMs species including Keggin,<sup>4</sup> wells-Dawson,<sup>5</sup> Lindqvist,<sup>6</sup> Anderson,<sup>7</sup> polyoxovanadates<sup>8</sup> and other POMs derivatives<sup>9</sup> have been introduced to the MOCs,

Department of Chemistry, Bohai University, Liaoning Province Silicon Materials Engineering Technology Research Centre, Jinzhou, 121000, P. R. China Fax: +86-416-3400158; Tel: +86-416-3400158; Email: wangxiuli@bhu.edu.cn

††Electronic Supplementary Information (ESI) available: IR, PXRD, TG, and additional figures. CCDC 1022773–1022777. For ESI and crystallographic data in CIF or other electronic format see DOI: 10.1039/b000000x

which play various structure-directing roles in the construction of diverse POMs-based complexes.<sup>10</sup>

Despite numerous successes in the syntheses of new diverse MOCs by controlling pH value,<sup>11</sup> reaction temperature,<sup>12</sup> synthesis technologies<sup>13</sup> and so on, there are still many difficulties in the basic understanding of these syntheses. In a synthesis process, some additional agents in the reaction system can induce the formation of crystals. There is a great deal of experimental evidence indicating that the additional agents can play a key role in selectively producing various structures.<sup>14</sup> Though the role and mechanism of these reagents have not been researched clearly, this is also a new strategy to synthesize novel MOCs.

Thus, in this work, 4-amino-1,2,4-triazole (4-atrz) was selected as the multidentate ligand to assemble with Cu(II) ion and various POMs at the presence of citric acid or boric acid as additional agents for constructing new MOCs, in order to investigate whether the combination of multinuclear clusters with diverse polyoxoanions could be realized, and to explore the role of acids in the formation of the target compounds. Five POM-based MOCs containing multinuclear Cu(II) clusters and four types of POMs were obtained:  $[\text{Cu}_3(4\text{-atrz})_8(\text{PMo}_{12}\text{O}_{40})_2(\text{H}_2\text{O})_2] \cdot 2\text{H}_2\text{O}$  (**1**),  $[\text{Cu}_2(4\text{-atrz})_6(\text{SiW}_{12}\text{O}_{40})(\text{H}_2\text{O})] \cdot 6\text{H}_2\text{O}$  (**2**),  $[\text{Cu}_2(4\text{-atrz})_4(\mu_2\text{-OH})(\text{CrMo}_6(\text{OH})_6\text{O}_{18})] \cdot 3\text{H}_2\text{O}$  (**3**),  $[\text{Cu}_3(4\text{-atrz})_3(\text{Mo}_8\text{O}_{27})(\text{H}_2\text{O})_4] \cdot 6\text{H}_2\text{O}$  (**4**) and  $[\text{Cu}_3(4\text{-atrz})_3(\text{V}_{10}\text{O}_{30})_{0.5}(\mu_3\text{-OH})(\text{H}_2\text{O})] \cdot \text{H}_2\text{O}$  (**5**). The effect of various polyoxoanions on the structures of the title compounds and the role of additional acid agents were discussed. Additionally, the photocatalytic activities of **1–5** were also investigated in detail.

## Experimental section

### Materials and methods

In this work,  $\text{Na}_3[\text{CrMo}_6(\text{OH})_6\text{O}_{18}] \cdot 8\text{H}_2\text{O}$  and  $(\text{NH}_4)_3[\text{CoMo}_6(\text{OH})_6\text{O}_{18}] \cdot 7\text{H}_2\text{O}$  were synthesized according to the literatures,<sup>15</sup> and other chemicals used for synthesis were of reagent grade and used without further purification. Elemental analyses (C, H and N) were performed on a Perkin–Elmer 240C elemental analyzer. FT-IR spectra were taken on a Varian 640 FT-IR spectrometer (KBr pellets). PXRD investigation was carried out with a Ultima IV with D/teX Ultra diffractometer at 40 kV, 40 mA with Cu  $K\alpha$  ( $\lambda = 1.5406 \text{ \AA}$ ) radiation. Thermogravimetric analyses (TGA) were performed on a SDT 2960 Simultaneous DSC-TGA instrument under flowing  $\text{N}_2$  atmosphere with a heating rate of  $10 \text{ }^\circ\text{C} \cdot \text{min}^{-1}$ . UV-Vis absorption spectra were measured using a SP-1901 UV-Vis spectrophotometer.

### Syntheses of 1–5

**Synthesis of  $[\text{Cu}_3(4\text{-atrz})_8(\text{PMo}_{12}\text{O}_{40})_2(\text{H}_2\text{O})_2] \cdot 2\text{H}_2\text{O}$  (**1**).** A mixture of  $\text{Cu}(\text{NO}_3)_2 \cdot 3\text{H}_2\text{O}$  (0.121 g, 0.5 mmol), 4-atrz (0.025 g, 0.3 mmol),  $\text{H}_3\text{PMo}_{12}\text{O}_{40}$  (0.183 g, 0.1 mmol), citric acid (0.021 g, 0.1 mmol) and  $\text{H}_2\text{O}$  (10 mL) was stirred for 30 min at room temperature. The initial pH value is 2.1. Then the mixture was sealed in a 25 mL Teflon reactor and heated at  $120 \text{ }^\circ\text{C}$  for 4 days. After slowly cooling to room temperature, green block crystals were filtered and washed with deionized water. Yield: 25% based on Cu. Elemental analyses: Calc. for  $\text{C}_{16}\text{H}_{40}\text{Cu}_3\text{N}_3\text{O}_{84}\text{P}_2\text{Mo}_{24}$

(4579.92): C 4.20, H 0.88, N 9.79 (%); found: C 4.35, H 0.85, N 9.71 (%). IR (KBr pellet,  $\text{cm}^{-1}$ ): 3447 (s), 3126 (w), 1589 (m), 1398 (w), 1217 (w), 1063 (s), 961 (s), 880 (m), 793 (s), 619 (s).

**Synthesis of  $[\text{Cu}_2(4\text{-atrz})_6(\text{SiW}_{12}\text{O}_{40})(\text{H}_2\text{O})] \cdot 6\text{H}_2\text{O}$  (**2**).** The synthesis procedure of **2** is similar to that of **1**, except that  $\text{H}_4\text{SiW}_{12}\text{O}_{40} \cdot 26\text{H}_2\text{O}$  (0.288 g, 0.1 mmol) was used instead of  $\text{H}_3\text{PMo}_{12}\text{O}_{40}$ . The initial pH value is 2.0. After slowly cooling to room temperature, blue block crystals were filtered and washed with deionized water. Yield: 32% based on Cu. Elemental analyses: Calc. for  $\text{C}_{12}\text{H}_{38}\text{Cu}_2\text{N}_{24}\text{O}_{47}\text{SiW}_{12}$  (3632.03): C 3.97, H 1.05, N 9.26 (%); found: C 4.05, H 0.99, N 9.20 (%). IR (KBr pellet,  $\text{cm}^{-1}$ ): 3345 (s), 3127 (m), 1618 (s), 1541 (m), 1398 (w), 1211 (s), 1082 (s), 974 (s), 922 (s), 793 (s), 623 (s).

**Synthesis of  $[\text{Cu}_2(4\text{-atrz})_4(\mu_2\text{-OH})(\text{CrMo}_6(\text{OH})_6\text{O}_{18})] \cdot 3\text{H}_2\text{O}$  (**3**).** A mixture of  $\text{Cu}(\text{NO}_3)_2 \cdot 3\text{H}_2\text{O}$  (0.121 g, 0.5 mmol), 4-atrz (0.084 g, 1 mmol),  $\text{Na}_3[\text{CrMo}_6(\text{OH})_6\text{O}_{18}] \cdot 8\text{H}_2\text{O}$  (0.123 g, 0.10 mmol) and  $\text{H}_2\text{O}$  (10 mL) was stirred for 30 min at room temperature. The initial pH value is 3.6. Then the mixture was sealed in a 25 mL Teflon reactor and heated at  $120 \text{ }^\circ\text{C}$  for 4 days. After slowly cooling to room temperature, blue block crystals were filtered and washed with deionized water. Yield: 57% based on Cu. Elemental analyses: Calc. for  $\text{C}_8\text{H}_{29}\text{Cu}_2\text{N}_{16}\text{O}_{28}\text{CrMo}_6$  (1552.19): C 6.19, H 1.88, N 14.44 (%); found: C 6.26, H 1.85, N 14.38 (%). IR (KBr pellet,  $\text{cm}^{-1}$ ): 3429 (m), 3111 (w), 1678 (m), 1624 (s), 1548 (s), 1217 (m), 1057 (m), 939 (s), 908 (s), 690 (s), 617 (s).

**Synthesis of  $[\text{Cu}_3(4\text{-atrz})_3(\text{Mo}_8\text{O}_{27})(\text{H}_2\text{O})_4] \cdot 6\text{H}_2\text{O}$  (**4**).** A mixture of  $\text{Cu}(\text{NO}_3)_2 \cdot 3\text{H}_2\text{O}$  (0.121 g, 0.5 mmol), 4-atrz (0.025 g, 0.3 mmol),  $(\text{NH}_4)_3[\text{CoMo}_6(\text{OH})_6\text{O}_{18}] \cdot 7\text{H}_2\text{O}$  (0.122 g, 0.1 mmol), citric acid (0.021 g, 0.1 mmol) and  $\text{H}_2\text{O}$  (10 mL) was stirred for 30 min at room temperature. The pH value of the mixture was adjusted to about 3.5 with  $1 \text{ mol} \cdot \text{L}^{-1}$  HCl. Then the mixture was sealed in a 25 mL Teflon reactor and heated at  $120 \text{ }^\circ\text{C}$  for 4 days. After slowly cooling to room temperature, green block crystals were filtered and washed with deionized water. Yield: 18% based on Cu. Elemental analyses: Calc. for  $\text{C}_6\text{H}_{32}\text{Cu}_3\text{N}_{12}\text{O}_{37}\text{Mo}_8$  (1822.58): C 3.95, H 1.77, N 9.22 (%); found: C 4.10, H 1.71, N 9.18 (%). IR (KBr pellet,  $\text{cm}^{-1}$ ): 3408 (m), 3132 (m), 1636 (s), 1558 (m), 1390 (m), 1229 (m), 1082 (s), 1022 (m), 935 (s), 833 (m), 619 (s), 468 (m).

**Synthesis of  $[\text{Cu}_3(4\text{-atrz})_3(\text{V}_{10}\text{O}_{30})_{0.5}(\mu_3\text{-OH})(\text{H}_2\text{O})] \cdot \text{H}_2\text{O}$  (**5**).** A mixture of  $\text{Cu}(\text{NO}_3)_2 \cdot 3\text{H}_2\text{O}$  (0.121 g, 0.5 mmol), 4-atrz (0.084 g, 1 mmol),  $\text{V}_2\text{O}_5$  (0.046 g, 0.25 mmol),  $\text{H}_3\text{BO}_3$  (0.093 g, 1.5 mmol) and  $\text{H}_2\text{O}$  (10 mL) was stirred for 30 min at room temperature. The pH value of the mixture was adjusted to about 5.0 with  $1 \text{ mol} \cdot \text{L}^{-1}$  NaOH. Then the mixture was sealed in a 25 mL Teflon reactor and heated at  $120 \text{ }^\circ\text{C}$  for 4 days. After slowly cooling to room temperature, green block crystals were filtered and washed with deionized water. Yield: 15% based on Cu. Elemental analyses: Calc. for  $\text{C}_6\text{H}_{17}\text{Cu}_3\text{N}_{12}\text{O}_{18}\text{V}_5$  (990.64): C 7.27, H 1.73, N 16.97 (%); found: C 7.35, H 1.68, N 16.89 (%). IR (KBr pellet,  $\text{cm}^{-1}$ ): 3412 (m), 3109 (m), 1624 (s), 1549 (m), 1400 (m), 1224 (s), 1078 (s), 916 (s), 812 (s), 683 (s), 465 (m).

### X-ray crystallography

X-ray diffraction data for **1–5** were collected on a Bruker SMART APEX II with Mo  $K\alpha$  ( $\lambda = 0.71073 \text{ \AA}$ ) by  $\omega$  and  $\theta$  scan

mode at 296 K. All the structures were solved by direct methods using the program SHELXS-97 and all non-hydrogen atoms were

**Table 1** Crystallographic data and structural refinements for **1–5**.

	<b>1</b>	<b>2</b>	<b>3</b>	<b>4</b>	<b>5</b>
Empirical formula	C <sub>16</sub> H <sub>40</sub> Cu <sub>3</sub> N <sub>32</sub> O <sub>84</sub> P <sub>2</sub> Mo <sub>24</sub>	C <sub>12</sub> H <sub>38</sub> Cu <sub>2</sub> N <sub>24</sub> O <sub>47</sub> SiW <sub>12</sub>	C <sub>8</sub> H <sub>29</sub> Cu <sub>2</sub> N <sub>16</sub> O <sub>28</sub> CrMo <sub>6</sub>	C <sub>6</sub> H <sub>32</sub> Cu <sub>3</sub> N <sub>12</sub> O <sub>37</sub> Mo <sub>8</sub>	C <sub>6</sub> H <sub>17</sub> Cu <sub>3</sub> N <sub>12</sub> O <sub>18</sub> V <sub>5</sub>
Formula weight	4579.92	3632.03	1552.19	1822.58	990.64
Crystal system	Monoclinic	Monoclinic	Triclinic	Monoclinic	Triclinic
Space group	<i>P</i> 2 <sub>1</sub> / <i>c</i>	<i>I</i> 2/ <i>a</i>	<i>P</i> -1	<i>P</i> 2 <sub>1</sub> / <i>c</i>	<i>P</i> -1
<i>a</i> (Å)	12.8229(4)	18.331(12)	13.4466(11)	10.0148(7)	8.7273(9)
<i>b</i> (Å)	14.7384(5)	13.2839(9)	13.4785(11)	19.0431(14)	12.8497(9)
<i>c</i> (Å)	25.0376(8)	26.055(2)	13.8805(12)	21.532(15)	12.8591(1)
$\alpha$ (°)	90	90	64.45(1)	90	86.154(1)
$\beta$ (°)	91.34(1)	109.215(1)	61.819(1)	102.757(1)	75.879(1)
$\gamma$ (°)	90	90	78.75(2)	90	75.844(1)
<i>V</i> (Å <sup>3</sup> )	4730.5(3)	5991.2(7)	2000.5(3)	4005.1(5)	1356.0(2)
<i>Z</i>	2	4	2	4	2
<i>D<sub>c</sub></i> (g cm <sup>-3</sup> )	3.215	4.026	2.577	3.023	2.426
$\mu$ (mm <sup>-1</sup> )	3.886	23.770	3.227	4.101	4.047
<i>F</i> (000)	4314	6452	1494	3484	966
Reflection collected	23459	15028	11694	20030	6986
Unique reflections	8336	5310	8262	7038	4762
<i>R</i> <sub>int</sub>	0.0167	0.0503	0.0282	0.0298	0.0183
GOF	1.044	1.063	1.023	1.045	1.062
<i>R</i> <sub><i>i</i></sub> <sup>a</sup> [ <i>I</i> > 2σ( <i>I</i> )]	0.0289	0.1225	0.0532	0.0370	0.0354
<i>wR</i> <sub>2</sub> <sup>b</sup> (all data)	0.1190	0.2838	0.1641	0.1054	0.1014

$$^a R_1 = \sum |F_o| - |F_c| / \sum |F_o|, \quad ^b wR_2 = \sum [w(F_o^2 - F_c^2)^2] / \sum [w(F_o^2)^2]^{1/2}.$$

refined anisotropically on F<sup>2</sup> by the full-matrix least-squares technique using the SHELXL-97 crystallographic software package.<sup>16</sup> The hydrogen atoms attached to water molecules with partial site occupancy or hydroxyl groups were not located in **1–5**. Some other restraints such as ‘ISOR’, ‘DFIX’, ‘EADP’ or ‘SIMU’ were also used in the refinements for obtaining more reasonable atom sites and thermal parameters. For compound **1**, the restraint command ‘ISOR’ was used to refine the non-H atom ‘O2W’ with ADP problem. For **2**, the restraint command ‘ISOR’ was used to refine the non-H atoms ‘C1, C2, C3, C4, C5, C6, N1, N2, N3, N4, N5, N6, N7, N8, N9, N10, N11, N12, O1W, O2W, O3W, O4W, Si1, O1, O2, O3, O4, O5, O6, O7, O8, O9, O10, O11, O12, O14, O15, O16, O17, O18, O19, O20, O21, O22’ with ADP problems, the command ‘DFIX’ was used to restrain the distances of N1 and N2, N3 and N4, N5 and N6 with longer bond lengths. In addition, the high *R*<sub>1</sub> and *wR*<sub>2</sub> factor of compound **2** might be due to the weak high-angle diffractions and the disordered atoms in the polyoxometalate. It was not possible to model the disordered solvent molecules appropriately. For compound **3**, the command ‘ISOR’ was used to refine atom N8 with ADP problem, and the command ‘DFIX’ was used to restrain the distance between N7 and N8 with longer bond length. For compound **4**, the restraint command ‘EADP’ was used to refine the non-H atoms ‘O1W, O5W’ with ADP problems, and command ‘SIMU’ was used to restrain all the O atoms with

similar thermal parameters. Relevant crystal data and structure refinements for **1–5** are listed in Table 1. Selected bond lengths (Å) and angles (°) for **1–5** are given in Table S1. Selected H-bonds of **1–4** are provided in Table S2–S5. Crystallographic data for **1–5** have been deposited in the Cambridge Crystallographic Data Center with CCDC reference numbers 1022773–1022777.

## Results and discussion

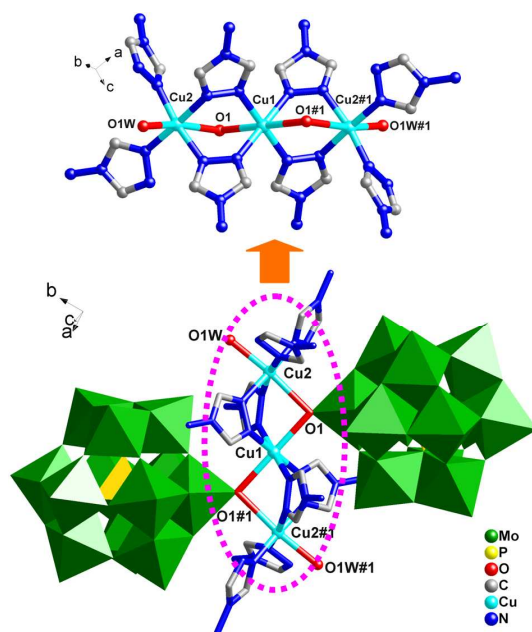
### Syntheses

Compounds **1–5** were synthesized by one pot procedure through reactions of Cu(NO<sub>3</sub>)<sub>2</sub>·3H<sub>2</sub>O, 4-atrz and various POMs in the presence of citric acid or boric acid under hydrothermal conditions. When H<sub>3</sub>PMo<sub>12</sub>O<sub>40</sub> or H<sub>4</sub>SiW<sub>12</sub>O<sub>40</sub>·26H<sub>2</sub>O was used as the reactant and citric acid was added in the reaction system, we harvested compounds **1** or **2**. However, we could only obtain some unknown precipitate without citric acid. When POM was replaced by Na<sub>3</sub>[CrMo<sub>6</sub>(OH)<sub>6</sub>O<sub>18</sub>]·8H<sub>2</sub>O at the presence of citric acid, a 1D complex Cu<sub>3</sub>(Mo<sub>8</sub>O<sub>26</sub>)(H<sub>2</sub>O)<sub>2</sub>(OH)<sub>2</sub>(4-atrz)<sub>4</sub> was obtained, which has been reported by Lin’s group through heating the mixture of CuCl<sub>2</sub>·2H<sub>2</sub>O, 4-atrz, Na<sub>2</sub>MoO<sub>4</sub>·2H<sub>2</sub>O and water at 160 °C for 3 days.<sup>17</sup> However, compound **3** was obtained at the absence of citric acid in this work. When (NH<sub>4</sub>)<sub>3</sub>[CoMo<sub>6</sub>(OH)<sub>6</sub>O<sub>18</sub>]·7H<sub>2</sub>O was used as the reactant and citric acid was also added, compound **4** was formed. While citric acid was not added, we also obtained

$\text{Cu}_3(\text{Mo}_8\text{O}_{26})(\text{H}_2\text{O})_2(\text{OH})_2(4\text{-atrz})_4$ . When POM and citric acid were replaced by  $\text{V}_2\text{O}_5$  and boric acid, respectively, compound **5** was generated. However, we did not get any crystal product except for some precipitate in the absence of boric acid. In addition, we also have explored the effect of these two acids on the formation of compounds **1–5**. Unfortunately, if we exchanged the two acids in the synthesis of **1–5**, only precipitate or poor crystals could be obtained. Although the citric acid or boric acid does not exist in the final structures of **1–5**, it can be concluded that citric acid or boric acid plays a key role in the formation of crystals **1–5** from the above results. We hypothesize that these acids presumably provide some templating role according to the experiments.

### Description of Crystal Structures

**[Cu<sub>3</sub>(4-atrz)<sub>8</sub>(PMo<sub>12</sub>O<sub>40</sub>)<sub>2</sub>(H<sub>2</sub>O)<sub>2</sub>]·2H<sub>2</sub>O (1)**. Single-crystal X-ray diffraction analysis reveals that compound **1** crystallizes in the monoclinic  $P2_1/c$  space group. Compound **1** consists of three Cu(II) ions, eight 4-atrz ligands, two [PMo<sub>12</sub>O<sub>40</sub>]<sup>3-</sup> anions (abbreviated as PMo<sub>12</sub>), two coordinated water molecules and two interstitial water molecules (Fig. 1). The PMo<sub>12</sub> heteropolyanion exhibits the well-known  $\alpha$ -Keggin-type structure. Valence sum calculations<sup>18</sup> show that all Mo atoms are in the +VI oxidation state, and all Cu atoms are in the +II oxidation state.



**Fig. 1** Structure of **1**: Coordination environments of the Cu(II) ions and the PMo<sub>12</sub> anions. All interstitial water molecules and H atoms are omitted for clarity. Symmetry codes: #1  $1-x, 2-y, 1-z$ .

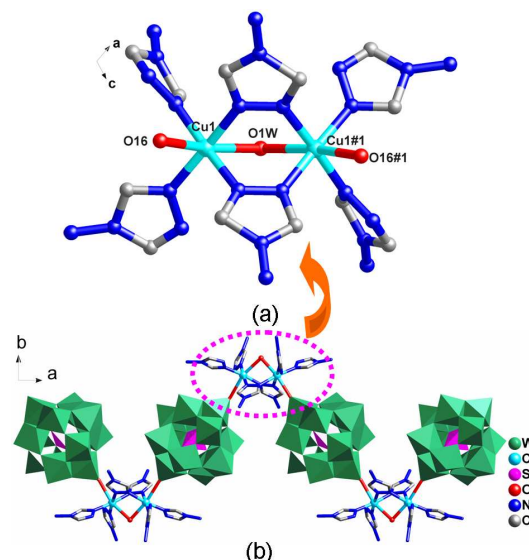
In **1**, there are two crystallographically independent Cu(II) ions (Cu1 and Cu2) (Table 2). The Cu1 ion, which lies on an inversion centre, is six-coordinated in an elongated octahedral geometry by four N atoms from four 4-atrz ligands and two O<sub>t</sub> atoms from two PMo<sub>12</sub> anions. The coordination sphere of Cu2 is composed of four N atoms from four 4-atrz ligands, one O atom of water molecule and one O<sub>t</sub> atom from one PMo<sub>12</sub> anion, exhibiting a distorted octahedral geometry. The Cu–O and Cu–N

bond lengths are in the range of 2.313(5)–2.590(2) and 1.980(5)–2.032(9) Å (Table S1).

Three Cu(II) ions (Cu1, Cu2 and Cu2#1) are bridged by eight 4-atrz ligands to construct a linear trinuclear cluster [Cu<sub>3</sub>(4-atrz)<sub>8</sub>]. Two PMo<sub>12</sub> anions provide a terminal oxygen atoms to coordinate with Cu1 and Cu2 ions, respectively, forming a [Cu<sub>3</sub>(4-atrz)<sub>8</sub>(PMo<sub>12</sub>O<sub>40</sub>)<sub>2</sub>(H<sub>2</sub>O)<sub>2</sub>] cluster. The [Cu<sub>3</sub>(4-atrz)<sub>8</sub>(PMo<sub>12</sub>O<sub>40</sub>)<sub>2</sub>(H<sub>2</sub>O)<sub>2</sub>] clusters are connected by the intermolecular hydrogen bonds [N(16)–H(16B)···O(27)] (Table S2) into a 2D supramolecular layer (Fig. S1a), which are further extended into a 3D supramolecular network (Fig. S1b) through another type of H-bonding interaction [N(12)–H(12B)···O(26)] (Table S2).

**[Cu<sub>2</sub>(4-atrz)<sub>6</sub>(SiW<sub>12</sub>O<sub>40</sub>)(H<sub>2</sub>O)]·6H<sub>2</sub>O (2)**. Compound **2** crystallizes in the monoclinic  $I2/a$  space group, which contains two Cu(II) ions, six 4-atrz ligands, one [SiW<sub>12</sub>O<sub>40</sub>]<sup>4-</sup> anion (abbreviated as SiW<sub>12</sub>), one coordinated water molecule which is on a twofold axis and six interstitial water molecules (Fig. 2). The SiW<sub>12</sub> anion in **2** is the classical Keggin-type heteropolyoxoanion, in which the Si1 atom is on an inversion centre. Valence sum calculations<sup>18</sup> show that all W atoms are in the +VI oxidation state, and all Cu atoms are in the +II oxidation state.

In **2**, there is only one crystallographically independent Cu(II) ion (Cu1). Cu1 is six-coordinated by four N atoms from four 4-atrz ligands, one O<sub>t</sub> atom from SiW<sub>12</sub> anion and one O1W atom to form distorted octahedral geometries (Table 2). The Cu–O and Cu–N bond lengths are in the range of 2.40(4)–2.46(8) Å and 1.96(3)–2.00(3) Å (Table S1). The adjacent Cu ions are bridged by six 4-atrz ligands and one water molecule to construct a binuclear Cu(II) cluster [Cu<sub>2</sub>(4-atrz)<sub>6</sub>(H<sub>2</sub>O)]. Each SiW<sub>12</sub> anion provides two terminal oxygen atoms to link the adjacent [Cu<sub>2</sub>(4-atrz)<sub>6</sub>(H<sub>2</sub>O)] clusters, forming a 1D zigzag chain (Fig. 2b).

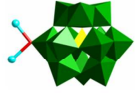
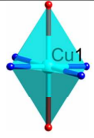
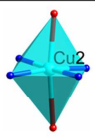
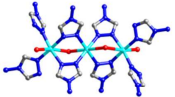
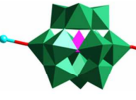
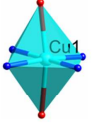
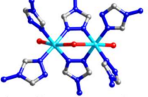

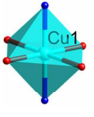
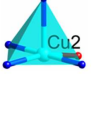
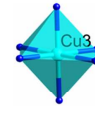
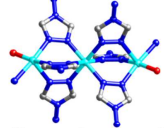
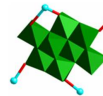
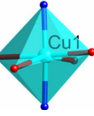
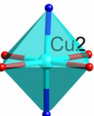
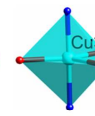
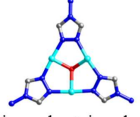
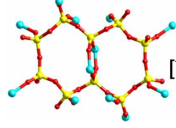
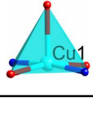
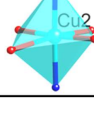
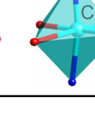
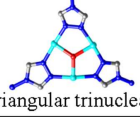


**Fig. 2** (a) Coordination environment of the Cu(II) ions in **2**, all interstitial water molecules and H atoms are omitted for clarity. (b) A view of 1D zigzag chain constructed from SiW<sub>12</sub> anions and binuclear [Cu<sub>2</sub>(4-atrz)<sub>6</sub>(H<sub>2</sub>O)] clusters. Symmetry codes: #1  $0.5-x, y, -z$ .

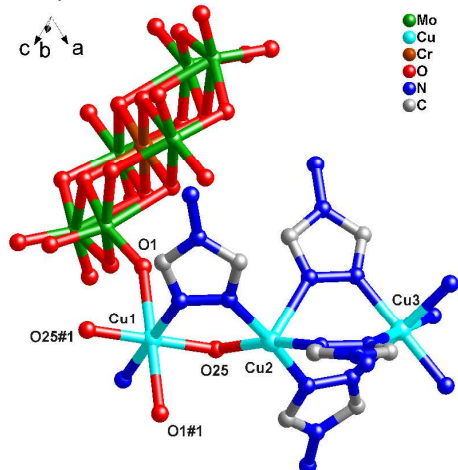
**[Cu<sub>2</sub>(4-atrz)<sub>4</sub>(μ<sub>2</sub>-OH)(CrMo<sub>6</sub>(OH)<sub>6</sub>O<sub>18</sub>)]·3H<sub>2</sub>O (3)**. Compound **3** crystallizes in the triclinic  $P-1$  space group. Compound **3**

consists of two Cu(II) ions, four 4-atrz ligands, one Anderson-type polyoxoanion  $[\text{CrMo}_6(\text{OH})_6\text{O}_{18}]^{3-}$  (abbreviated as  $\text{CrMo}_6$ ), one hydroxyl group and three interstitial water molecules (Fig. 3). The  $\text{CrMo}_6$  anion in **3** exhibits the classical B-type Anderson

**Table 2** Coordination Sites of POMs, coordination geometries of Cu(II) ions and the polynuclear Cu(II) clusters in **1–5**.

Compounds	Coordination sites of POMs	Coordination geometries of Cu(II) ions	The polynuclear Cu(II) clusters
Compound 1	 $[\text{PMo}_{12}]$	 Cu1  Cu2	 The linear trinuclear cluster
Compound 2	 $[\text{SiW}_{12}]$	 Cu1	 The dinuclear cluster
Compound 3	 $[\text{CrMo}_6]$	 Cu1  Cu2  Cu3	 The linear trinuclear cluster
Compound 4	 $[\text{Mo}_8\text{O}_{27}]$	 Cu1  Cu2  Cu3	 The triangular trinuclear cluster
Compound 5	 $[\text{V}_{10}\text{O}_{30}]$	 Cu1  Cu2  Cu3	 The triangular trinuclear cluster

structure. The heteroatom Cr forms an octahedron with six OH groups, and six  $[\text{MoO}_6]$  octahedrons arrange hexagonally around the central  $[\text{Cr}(\text{OH})_6]$  octahedron through sharing edges. Valence sum calculations<sup>18</sup> show that all Mo atoms are in the +VI oxidation state, and all Cu atoms are in the +II oxidation state.



**Fig. 3** Coordination environments of the Cu(II) ions and  $\text{CrMo}_6$  anion in **3**. All interstitial water molecules and H atoms are omitted for clarity. Symmetry codes: #1  $1-x, -y, 1-z$ .

In **3**, there exist three crystallographically independent Cu(II) ions (Cu1, Cu2 and Cu3), which show different coordination geometries (Table 2). The Cu1 ion lies on an inversion centre. The octahedral geometry of Cu1 consists of two hydroxyl O atoms and two  $\text{O}_1$  atoms from  $\text{CrMo}_6$  as the basal plane, and two

N atoms from two 4-atrz ligands as vertex. Cu2 is five-coordinated by four N atoms from four 4-atrz ligands and one hydroxyl O atom, forming distorted rectangular pyramidal geometry. Cu3 locates in an octahedral geometry, which is defined by six N atoms from six 4-atrz ligands. The Cu–O and Cu–N bond lengths are in the range of 1.945(6)–2.397(7) Å and 1.980(8)–2.447(9) Å (Table S1). Cu2 and Cu3 are linked by six 4-atrz ligands with their adjacent N atoms to generate a linear trinuclear Cu(II) cluster  $[\text{Cu}_3(4\text{-atzr})_6]$ . The linear trinuclear Cu(II) clusters and Cu1 ions are connected alternately by adjacent N atoms of 4-atrz and hydroxyl groups to produce a 1D linear chain. The  $\text{CrMo}_6$  anions coordinate to Cu1 ions as the monodentate ligands hanging on both sides of the 1D chain (Fig. 4). The 1D chains are connected by hydrogen bonding interactions  $[\text{N}(12)\text{--H}(12\text{A})\cdots\text{O}(6), 2.994 \text{ \AA}]$  (Table S3) between 4-atrz and  $\text{CrMo}_6$  anions, constructing a 2D supramolecular layer (Fig. S2a). The adjacent 2D layers are further connected by another type of H-bond  $[\text{C}(5)\text{--H}(5)\cdots\text{O}(9), 3.131 \text{ \AA}]$  (Table S3) to form a 3D supramolecular skeleton (Fig. S2b).

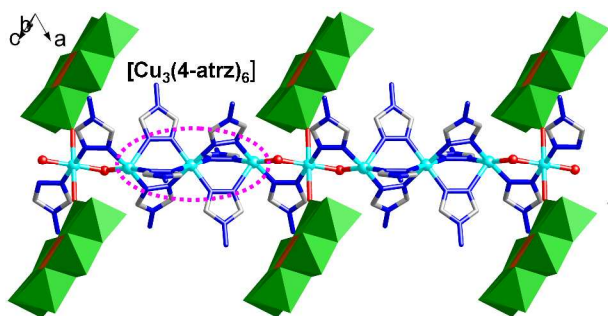


Fig. 4 View of 1D infinite chain based on trinuclear  $[\text{Cu}_3(4\text{-atrz})_6]$  clusters and  $\text{CrMo}_6$  anions in **3**.

$[\text{Cu}_3(4\text{-atrz})_3(\text{Mo}_8\text{O}_{27})(\text{H}_2\text{O})_4] \cdot 6\text{H}_2\text{O}$  (**4**). Compound **4** crystallizes in the triclinic  $P2_1/c$  space group and consists of three crystallographically independent Cu(II) ions, three 4-atrz ligands, one  $\gamma$ -octamolybdate  $[\text{Mo}_8\text{O}_{27}]^{6-}$  polyoxoanion, four coordinated water molecules and six interstitial water molecules (Fig. 5). Valence sum calculations<sup>18</sup> show that all Mo atoms are in the +VI oxidation state, and all Cu atoms are in the +II oxidation state.

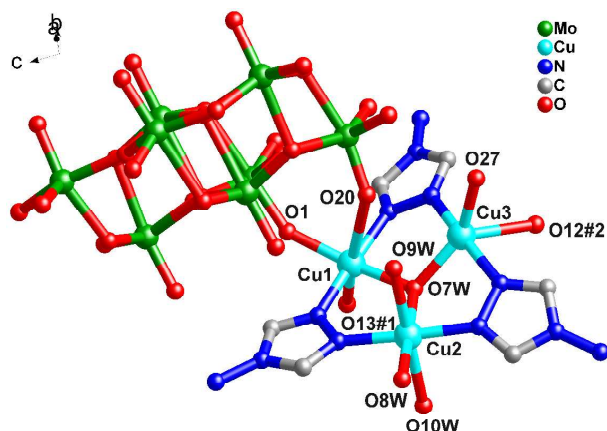


Fig. 5 Coordination environment of the Cu(II) ions in **4**. All interstitial water molecules and H atoms are omitted for clarity. Symmetry codes: #1  $-1 + x, y, z$ ; #2  $-1 + x, 0.5 - y, -0.5 + z$ .

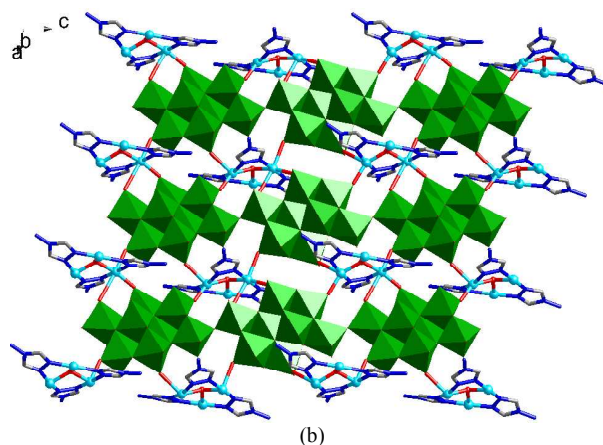
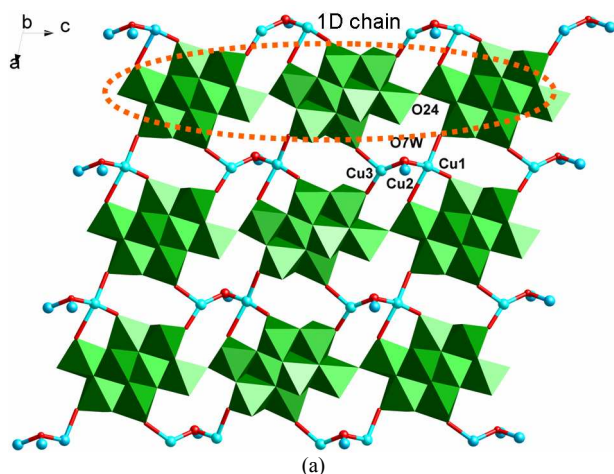


Fig. 6 (a) View of 2D layer of **4** containing infinite  $[\text{Mo}_8\text{O}_{27}]^{6-}$  chains. (b) The 2D network constructed from the  $[\text{Mo}_8\text{O}_{27}]^{6-}$  chains and the trinuclear clusters.

Cu1 and Cu2 have similar octahedral geometries (Table 2). Cu1 is six-coordinated by three O atoms from  $[\text{Mo}_8\text{O}_{27}]^{6-}$  anions, two N atoms from two 4-atrz ligands and one O atom of coordinated water molecule. Cu2 is defined by two N atoms from two 4-atrz ligands and four O atoms of four coordinated water molecules. While Cu3 locates at trigonal bipyramid geometry, which is five-coordinated by two O atoms from  $[\text{Mo}_8\text{O}_{27}]^{6-}$  anions, two N atoms from two 4-atrz ligands and one O atom of coordinated water molecule. The Cu–O and Cu–N bond lengths are in the range of 1.946(5)–2.782(5) Å and 1.945(6)–1.993(6) Å (Table S1), respectively. The three Cu(II) ions are linked by three 4-atrz ligands with adjacent N atoms and O7W to form an approximate trigonal planar trinuclear cluster  $[\text{Cu}_3(4\text{-atrz})_3(\text{H}_2\text{O})]$ .

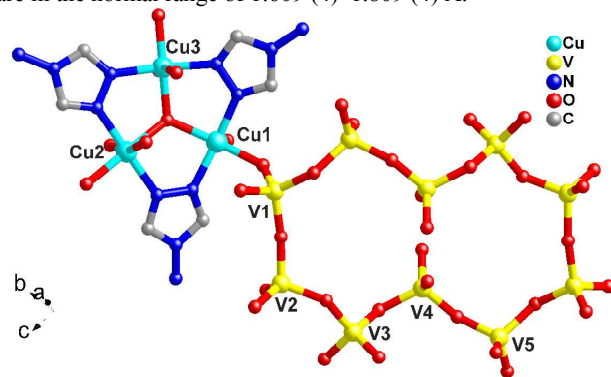
The  $[\text{Mo}_8\text{O}_{27}]^{6-}$  anion is built up from  $[\text{Mo}_8\text{O}_{28}]^{8-}$  subunit, composed of eight edge-shared distorted  $[\text{MoO}_6]$  octahedrons. The  $[\text{Mo}_8\text{O}_{28}]^{8-}$  blocks condense *via* sharing one common vertex (O24) to form infinite  $[\text{Mo}_8\text{O}_{27}]^{6-}$  chains (Fig. 6a). Such an octamolybdate chain is rarely observed in the literatures.<sup>19</sup> It is worth mentioning that the  $[\text{CoMo}_6(\text{OH})_6\text{O}_{18}]^{3-}$  precursor is used as raw material in our synthesis reaction, and then the  $\text{CoMo}_6$  units are dissociated and reassembled to the  $[\text{Mo}_8\text{O}_{27}]^{6-}$  chains during reaction. To our knowledge, *in situ* synthesis and transformation of POMs is no longer unusual. For example, Cao's group<sup>20</sup> uses  $\text{Na}_2\text{WO}_4$  and  $\text{H}_3\text{PO}_4$  as raw material to induce *in situ* synthesis of three types of POMs, namely,  $[\text{PW}_{12}\text{O}_{40}]^{3-}$ ,  $[\text{P}_2\text{W}_{18}\text{O}_{62}]^{6-}$  and  $[\text{PW}_{10}\text{Ag}_2\text{O}_{39}]^{11-}$ . Niu's group<sup>21</sup> prepares a Wells–Dawson  $[\text{P}_2\text{Mo}_{18}\text{O}_{62}]^{6-}$ -based compound using Keggin specie  $\text{H}_3\text{PMo}_{12}\text{O}_{40}$  as starting materials. Our group<sup>22</sup> also obtained lacunary  $[\text{PW}_9\text{O}_{34}]^{9-}$  unit with Keggin  $\text{H}_3\text{PW}_{12}\text{O}_{40}$  as raw material. However, this transformation from Anderson-type  $\text{CoMo}_6$  unit to  $\text{Mo}_8\text{O}_{27}$  has not been reported up to now.

The  $\text{Mo}_8\text{O}_{27}$  infinite chains are linked by the trinuclear  $[\text{Cu}_3(4\text{-atrz})_3(\text{H}_2\text{O})]$  clusters form 2D networks (Fig. 6b), which are further extended into a 3D supramolecule framework (Fig. S3) by H-bonding interactions  $[\text{N}(8)\text{--H}(8\text{A})\cdots\text{O}(16)]$ , 2.910 Å] (Table S4).

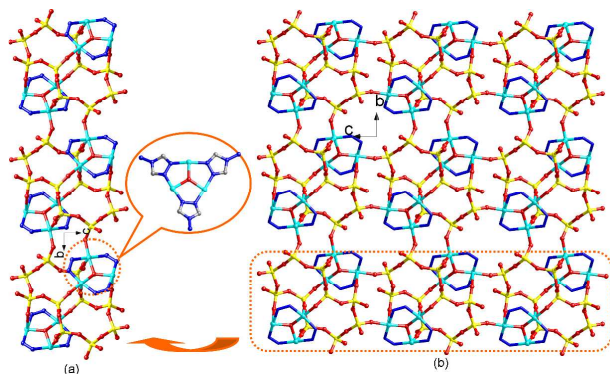
$[\text{Cu}_3(4\text{-atrz})_3(\text{V}_{10}\text{O}_{30})_{0.5}(\mu_3\text{-OH})(\text{H}_2\text{O})] \cdot \text{H}_2\text{O}$  (**5**). Compound **5** crystallizes in the triclinic  $P-1$  space group and is composed of three Cu(II) ions, three 4-atrz ligands, half of  $[\text{V}_{10}\text{O}_{30}]^{10-}$  ring, one hydroxyl group, one coordinated water molecule and one interstitial water molecule (Fig. 7). Valence sum calculations<sup>18</sup>

show that all V atoms are in the +V oxidation state, and all Cu atoms are in the +II oxidation state. Cu1 is five-coordinated by three O atoms from a  $\mu_3$ -hydroxyl group and two  $[\text{V}_{10}\text{O}_{30}]^{10-}$  rings and two N atoms from two 4-atrz ligands, generating a rectangular pyramid geometry. Both Cu2 and Cu3 exhibit similar octahedral geometries. The coordination sphere of Cu2 is defined by two O atoms from two  $[\text{V}_{10}\text{O}_{30}]^{10-}$  rings, a  $\mu_3$ -hydroxyl group and one water molecule as the basal plane, and two N atoms from two 4-atrz ligands as the vertexes. The Cu3 is also six-coordinated by three O atoms from two  $[\text{V}_{10}\text{O}_{30}]^{10-}$  rings, a  $\mu_3$ -hydroxyl and two N atoms from two 4-atrz ligands. The Cu–O and Cu–N bond lengths are in the range of 1.936(3)–2.659(2) Å and 1.966(4)–1.991(4) Å (Table S1), respectively. Similarly to **4**, three Cu(II) ions are linked by three 4-atrz ligands with adjacent N atoms and a  $\mu_3$ -OH to form a trigonal planar trinuclear cluster  $[\text{Cu}_3(4\text{-atrz})_3(\text{OH})]$ .

It is worthy of being noted that there exists a macrocyclic polyoxovanadate  $[\text{V}_{10}\text{O}_{30}]^{10-}$  ring in **5**, in which ten tetrahedral  $\text{VO}_4$  units are interlinked through sharing vertexes, and the  $[\text{V}_{10}\text{O}_{30}]^{10-}$  ring lies an inversion centre (Fig. 7). As far as we know, this kind of  $[\text{V}_{10}\text{O}_{30}]^{10-}$  ring is very limited in the literatures, and only Hayashi's group reported a series of  $[\text{V}_{10}\text{O}_{30}]^{10-}$  ring-based lanthanide inorganic compounds and two transition metal inorganic compounds.<sup>23</sup> The V–O bond lengths are in the normal range of 1.609 (4)–1.809 (4) Å.

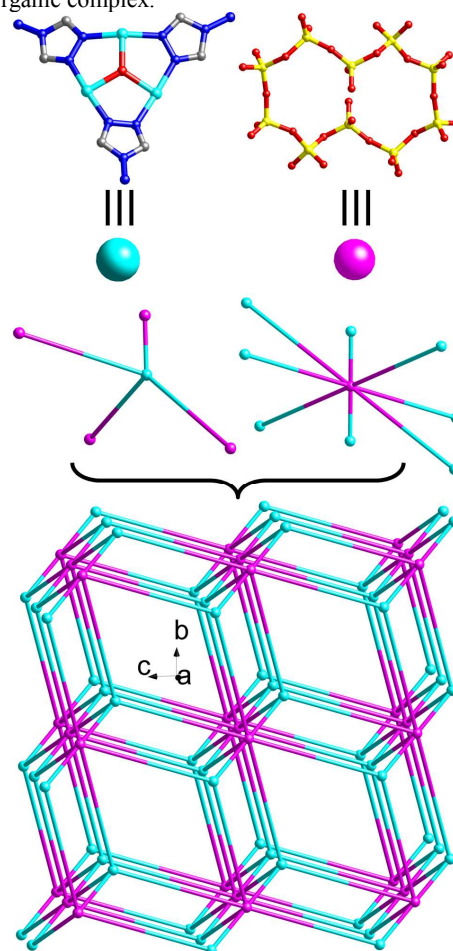


**Fig. 7** The  $[\text{V}_{10}\text{O}_{30}]^{10-}$  ring and the coordination environments of the Cu(II) ions in **5**. All interstitial water molecules and H atoms are omitted for clarity.



**Fig. 8** The 2D network constructed by trinuclear  $[\text{Cu}_3(4\text{-atrz})_3(\text{OH})]$  clusters and  $[\text{V}_{10}\text{O}_{30}]^{10-}$  rings alternatively. All uncoordinated N atoms and C atoms are omitted for clarity.

As is shown in Fig. 8, the  $[\text{Cu}_3(4\text{-atrz})_3(\text{OH})]$  clusters connected with the  $[\text{V}_{10}\text{O}_{30}]^{10-}$  rings to construct a 2D network, in which each  $[\text{Cu}_3(4\text{-atrz})_3(\text{OH})]$  cluster connected with three  $[\text{V}_{10}\text{O}_{30}]^{10-}$  rings and each  $[\text{V}_{10}\text{O}_{30}]^{10-}$  ring connected with six  $[\text{Cu}_3(4\text{-atrz})_3(\text{OH})]$  clusters. The adjacent 2D networks are linked by the coordination bonds between the Cu ions and O atoms from  $[\text{V}_{10}\text{O}_{30}]^{10-}$  rings to form a 3D metal organic framework (Fig. S4). From topological viewpoint, each  $[\text{Cu}_3(4\text{-atrz})_3(\text{OH})]$  cluster links four  $[\text{V}_{10}\text{O}_{30}]^{10-}$  rings, which can be regarded as a four-connected node. Each  $[\text{V}_{10}\text{O}_{30}]^{10-}$  ring connected with eight  $[\text{Cu}_3(4\text{-atrz})_3(\text{OH})]$  clusters, acting as an eight-connected node. Thus, compound **5** shows a 3D (4, 8)-connected topology with  $\{4^6 \cdot 6^{12} \cdot 8^4\} \{4^6\}_2$  Schläfli symbol (Fig. 9). To our knowledge, compound **5** represents the first example of  $\text{V}_{10}\text{O}_{30}$ -based 3D metal-organic complex.



**Fig. 9** Representation of 3D binodal (4, 8)-connected topology of **5**.

### The effect of polyoxoanions on the polynuclear Cu(II) clusters and the final structures of **1–5**

In this work, four types of POMs have been used as structure-directing building blocks and five metal-organic complexes with diverse structures have been obtained. Another structural feature of **1–5** is the formation of four types of polynuclear Cu(II) clusters at the presence of 4-atrz ligand and various POMs, as shown in Table 2. In **1**, Keggin-type  $\text{PMo}_{12}$  anion was used as the inorganic building unit to assemble with Cu(II) ions and 4-atrz



ligand, a 0D  $\text{PMo}_{12}$ -based complex containing linear trinuclear clusters  $[\text{Cu}_3(4\text{-atrz})_8(\text{H}_2\text{O})_2]$  was constructed. The  $\text{PMo}_{12}$  anion provides an oxygen atom to coordinate with two Cu(II) ions from a trinuclear cluster, which did not play the linking role to extend the structure. When Keggin-type  $\text{SiW}_{12}$  anion was introduced to the same reaction system in **2**, a 1D zigzag chain containing linear dinuclear  $[\text{Cu}_2(4\text{-atrz})_6(\text{H}_2\text{O})]$  clusters has been obtained, in which each  $\text{SiW}_{12}$  polyanion provides two oxygen atoms acting as linkers to connect the dinuclear clusters. In compound **3**,  $\text{CrMo}_6$  was employed as the structure-directing agent, an infinite 1D chain based on linear trinuclear  $[\text{Cu}_3(4\text{-atrz})_6]$  clusters is constructed. The  $\text{CrMo}_6$  polyanions hang on both sides of the chain as monodentate ligands. When  $\text{CoMo}_6$  was introduced to the reaction system, a triangular trinuclear  $[\text{Cu}_3(4\text{-atrz})_3(\text{H}_2\text{O})]$  cluster was formed in **4**, and the  $\text{CoMo}_6$  was transformed to  $\text{Mo}_8\text{O}_{27}$  anion. Finally, a 2D network was constructed from the trinuclear  $[\text{Cu}_3(4\text{-atrz})_3(\text{H}_2\text{O})]$  clusters and the rare 1D  $\text{Mo}_8\text{O}_{27}$  inorganic chains. In compound **5**,  $\text{V}_2\text{O}_5$  was used as the reactant, a 3D (4, 8)-connected framework constructed from the  $\text{V}_{10}\text{O}_{30}$  polyanion rings and triangular trinuclear  $[\text{Cu}_3(4\text{-atrz})_3(\text{OH})]$  clusters was generated. By comparing the structures of **1–5**, it is found that the linear multinuclear Cu(II) clusters could be constructed at the presence of heteropolyanions, which might result in the lower dimensional compounds (**1–3**), while the triangular trinuclear Cu(II) clusters could be formed at the presence of isopolyanions, which might induce the formation of higher dimensional compounds (**4–5**). Thus, we can conclude that the polyanions play an important structure-directing role in the construction of polynuclear clusters as well as the final structures.

### 30 IR spectra and PXRD

The IR spectra of **1–5** are shown in Fig. S5. In the spectrum of **1**, the bands at 961, 880, 793 and  $1063\text{ cm}^{-1}$  could be ascribed to the characteristic peaks of  $\nu_{\text{as}}(\text{Mo}-\text{O}_t)$ ,  $\nu_{\text{as}}(\text{Mo}-\text{O}_b-\text{Mo})$ ,  $\nu_{\text{as}}(\text{Mo}-\text{O}_c-\text{Mo})$  and  $\nu_{\text{as}}(\text{P}-\text{O})$ .<sup>24</sup> For **2**, the characteristic peaks at 974, 922, 793 and  $1082\text{ cm}^{-1}$  are attributed to  $\nu_{\text{as}}(\text{W}-\text{O}_t)$ ,  $\nu_{\text{as}}(\text{W}-\text{O}_b-\text{W})$ ,  $\nu_{\text{as}}(\text{W}-\text{O}_c-\text{W})$  and  $\nu_{\text{as}}(\text{Si}-\text{O})$ .<sup>25</sup> The characteristic bands at 690, 908,  $939\text{ cm}^{-1}$  for **3** are attributed to  $\nu(\text{Mo}-\text{O}_t)$ ,  $\nu(\text{Mo}-\text{O}_c)$  and  $\nu(\text{Mo}-\text{O}_b)$ .<sup>15a</sup> For **4**, the bands at 935, 833, 619 and  $468\text{ cm}^{-1}$  are assigned to  $\nu(\text{Mo}-\text{O}_t)$  and  $\nu(\text{Mo}-\text{O}_b-\text{Mo})$ .<sup>26</sup> In **5**, the bands at 1078, 916, 812, 683 and  $465\text{ cm}^{-1}$  correspond to the V–O stretches.<sup>23d</sup> In addition, the bands in the  $1000\text{--}1700\text{ cm}^{-1}$  region can be assigned to the characteristic peaks of 4-atrz ligand, and the weak broad bands at  $3100\text{--}3500\text{ cm}^{-1}$  should be attributed to the vibration of  $\nu(\text{OH})$  of water molecules or hydroxyl groups.<sup>27</sup>

The PXRD patterns for **1–5** are shown in Fig. S6. The diffraction peaks of both simulated and experimental patterns match well in the key positions, which indicate the phase purities of **1–5**. The different intensity may be derived from the variation in preferred orientation of the powder samples during the collection of data.<sup>28</sup>

### Thermal stability

Thermal stability of compounds **1–5** was checked in the temperature range from room temperature to  $800^\circ\text{C}$  with a heating rate of  $10^\circ\text{C}\cdot\text{min}^{-1}$  under  $\text{N}_2$  atmosphere.

Thermogravimetric analyses indicate all compounds exhibit two main weight loss steps (Fig. S7). The TGA curve of **1** shows the thermal stability up to  $172^\circ\text{C}$ , and then the weight loss of 1.56% in the range of 172 to  $238^\circ\text{C}$  is attributed to the release of two interstitial water molecules and two coordinated water molecules (calcd 1.57%). Compound **2** shows a weight loss of 2.62% below  $145^\circ\text{C}$  corresponding to the decrease of six interstitial water molecules (calcd 2.97%), and the coordinated water molecule should be lost in the second weight loss. The first weight loss of **3** is 6.99%, which may be resulted from the loss of three interstitial water molecules (calcd 3.48%) and partial hydroxyl groups. Compound **4** starts to lose its weight at the beginning of heating with a weight loss of 9.02%, due to the loss of six interstitial water molecules and four coordinated water molecules (calcd 9.88%). Compound **5** loses 2.63% of weight below  $117^\circ\text{C}$  corresponding to the loss of one interstitial water molecule (calcd 1.82%), and the coordinated water molecule and the coordinated hydroxyl group also should be assigned to the second weight loss. The second weight loss of **1–5** represents the decomposition of the remaining structures.

### Photocatalytic Activity

It's well-known that some POMs-based MOCs could be used as green photocatalysts for the removal of organic pollutants from water.<sup>29</sup> During the photocatalytic process of POM-based MOCs, UV-vis light induces POM/organic ligands to produce oxygen and/or nitrogen–metal charge transfer by promoting an electron from the highest occupied molecular orbital (HOMO) to the lowest unoccupied molecular orbital (LUMO). The HOMO strongly demands one electron to return to its stable state. Therefore, one electron was captured from water molecules, which were oxygenated into the  $\bullet\text{OH}$  active species, to complete the photocatalytic process.<sup>30</sup> Methylene blue (MB), rhodamine B (RhB) and methyl orange (MO) are the most common organic dyes in waste water, therefore they were selected as model pollutants to investigate their degradation in the presence of **1–5** in this work. The photocatalytic reactions were performed by a typical process<sup>31</sup>: 150 mg of **1**, **2**, **3**, **4** or **5** was dispersed in 90 mL aqueous solution of MB ( $6\text{ mg L}^{-1}$ ), MO ( $6\text{ mg L}^{-1}$ , pH ~ 2.5) or RhB ( $6\text{ mg L}^{-1}$ ) under UV lamp, respectively. Before turning on the Hg lamp (125 W), the mixture containing organic dye and title compound was magnetically stirred in the dark for 30 min till an adsorption-desorption equilibrium was established. Then 5 mL samples were taken out regularly from the photocatalytic reactor and centrifuged immediately for separation of any solid. The transparent solution was tested for UV measurement.

The photocatalytic behaviors of **1–5** in MB solution are shown in Fig. 10a–c and Fig S8. Moreover, the concentration ratios of MB ( $c/c_0$ ) against irradiation time (min) in the presence of the title compounds were plotted, with  $c_0$  representing the initial concentration of MB after magnetically stirring in the dark for 30 min (Fig. 10d). It can be clearly seen that the absorbance peaks of MB decreased obviously along with the reaction time in the presence of **1–3**, but their photocatalytic efficiency is different. For **1**, the MB solution has been taken out every 5 min, and 96.52% of MB decomposes after 35 min of irradiation. For **2**, the MB solution has been taken out every 10 min, and 98.22% of MB decomposes after 60 min of irradiation. For **3**, the MB

solution has been taken out every 20 min, and 98.04% of MB decomposes after 140 min of irradiation. By comparison, the order of photocatalytic activity is  $1 > 2 > 3$ . While compounds 4 and 5 haven't shown obvious photocatalytic activity toward the degradation of MB during 180 min with the degradation rate of 13.14% and 9.31%, respectively.

The photocatalytic behaviors of 1–5 in RhB solution are shown in Fig. 11 and Fig. S9. The absorbance peaks of RhB solution decreased obviously along with the reaction time at the presence of compound 1 rather than compounds 2–5. The degradation ratios of RhB are 93.72 % for 1, 28.76 % for 2, 20.08 % for 3, 16.57 % for 4 and 3.91 % for 5 after 180 min of UV irradiation. The photocatalytic behaviors of 1–5 in MO solution are shown in Fig. S10. Obviously, compounds 1–5 show no photocatalytic effect on the degradation of MO.

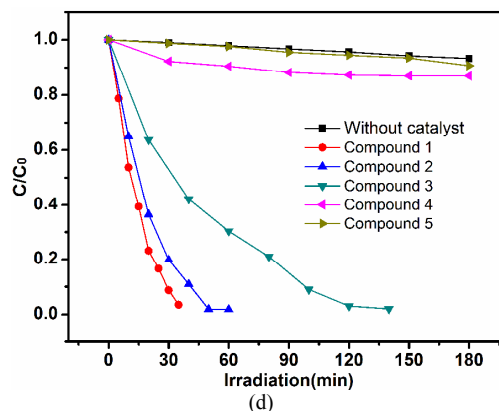
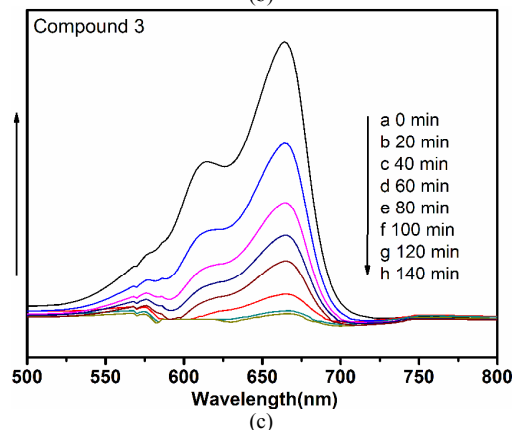
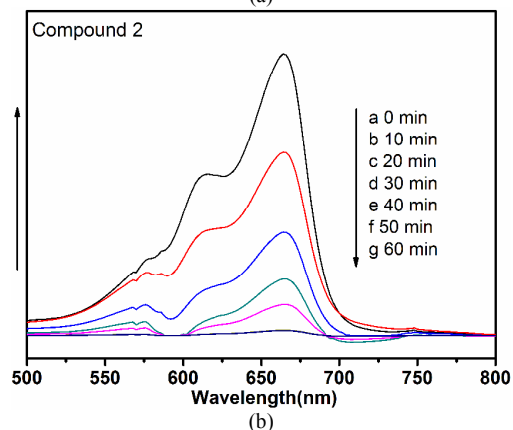
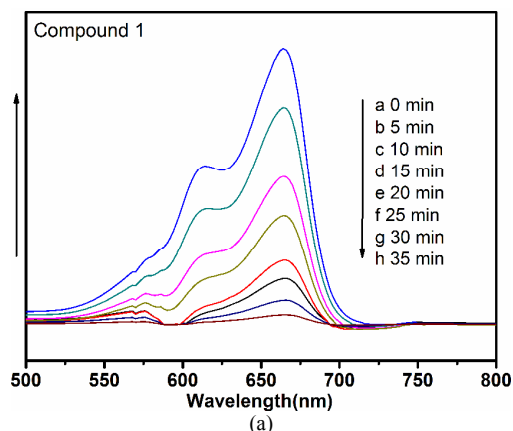


Fig. 10 Absorption spectra of the MB solution (a–c) in the presence of 1–3; (d) Plots of concentration ratios of MB ( $c/c_0$ ) against irradiation time (min) in the presence of 1–5 and without any catalyst during the decomposition reaction under UV irradiation.

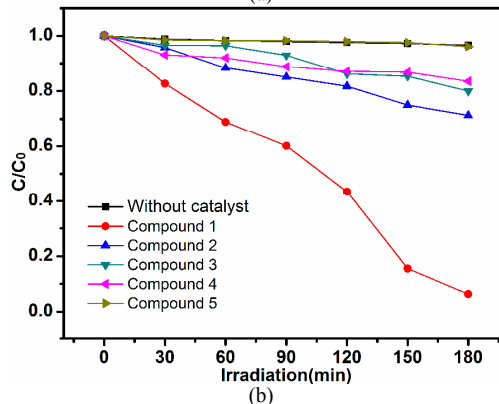
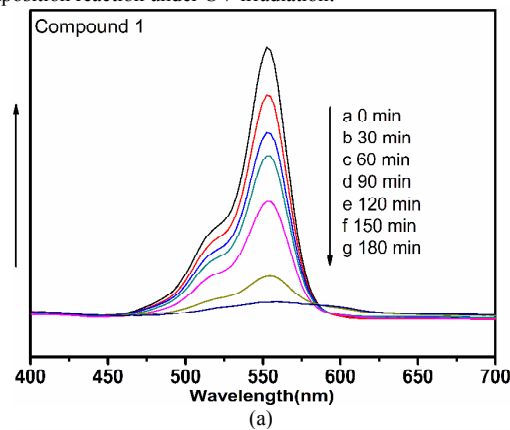


Fig. 11 (a) Absorption spectra of the RhB solution in the presence of 1; (b) Plots of concentration ratios of RhB ( $c/c_0$ ) against irradiation time (min) in the presence of 1–5 and without any catalyst during the decomposition reaction under UV irradiation.

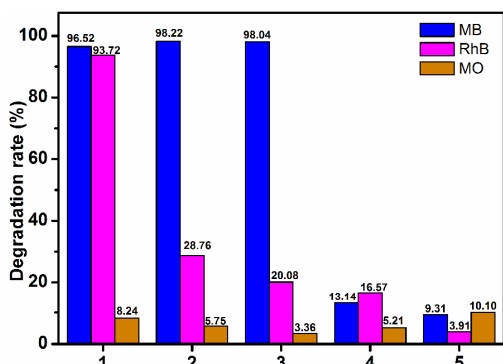


Fig. 12 Degradation rates of the MB, RhB and MO solutions in the presence of 1–5.

The degradation rates of MB, RhB and MO in the presence of 5 1–5 after UV irradiation are shown in Fig. 12. The results demonstrate that compounds 1–3 are good candidates for the photocatalytic degradation of MB and compound 1 is a good photocatalyst for the degradation of RhB. In addition, we measured the PXRD of 1–5 after the photocatalytic experiments, 10 and the PXRD patterns are nearly identical to the corresponding ones of the original compounds (Fig. S6), which indicate that compounds 1–5 are stable after photocatalytic reactions.

## Conclusions

In summary, by introducing four types of POMs into Cu(II)-4- 15 atrz reaction system at the presence of citric acid or boric acid or not, five POM-based MOCs containing various multinuclear clusters have been successfully prepared, which show diverse structures ranging from 0D trinuclear cluster, 1D chain, 2D network, to 3D framework. In 4, the  $\text{Mo}_8\text{O}_{27}$  unit is *in situ* 20 synthesized from Anderson-type  $\text{CoMo}_6$  raw materials. Compound 5 represents the first example of  $\text{V}_{10}\text{O}_{30}$ -based 3D metal–organic complex. The POMs play an important structure-directing role in the construction of title compounds and show great effect on the structures of 1–5. The citric acid and boric 25 acid play a key role in the assembly of title compounds, which suggest an effective strategy in crystal engineering for preparing new POM-based MOCs. Compounds 1–3 exhibit good photocatalytic activity and selectivity for the degradation of some organic dyes.

## Acknowledgements

This work was supported by the National Natural Science Foundation of China (Nos. 21171025, 21471021 and 21201021), Program for New Century Excellent Talents in University (NCET-09-0853) and Program of Innovative Research Team in 35 University (LT2012020).

## Notes and references

- (a) X. L. Wang, N. Li, A. X. Tian, J. Ying, T. J. Li, X. L. Lin, J. Luan, and Y. Yang, *Inorg. Chem.*, 2014, **53**, 7118; (b) Y. Z. Gao, Y. Q. Xu, K. L. Huang, Z. G. Han and C. W. Hu, *Dalton Trans.*, 2012, **41**, 6122; 40 (c) H. Fu, C. Qin, Y. Lu, Z. M. Zhang, Y. G. Li, Z. M. Su, W. L. Li and E. B. Wang, *Angew. Chem.*, 2012, **124**, 1; (d) F. J. Ma, S. X. Liu, C. Y. Sun, D. D. Liang, G. J. Ren, F. Wei, Y. G. Chen, and Z. M. Su, *J. Am. Chem. Soc.*, 2011, **133**, 4178; (e) X. J. Feng, W. Z. Zhou, Y. G. Li, H. S. Ke, J. K. Tang, R. Clérac, Y. H. Wang, Z. M.

- Su and E. B. Wang, *Inorg. Chem.*, 2012, **51**, 2722; (f) Q. X. Han, L. J. Zhang, C. He, J. Y. Niu and C. Y. Duan, *Inorg. Chem.*, 2012, **51**, 5118.
- 2 (a) D. L. Long, E. Burkholder and L. Cronin, *Chem. Soc. Rev.*, 2007, **36**, 105; (b) A. Müller, P. Kögerler and A. W. M. Dress, *Coord. Chem. Rev.*, 2001, **222**, 193; (c) R. M. Yu, X. F. Kuang, X. Y. Wu, C. Z. Lu, *Coord. Chem. Rev.*, 2009, **253**, 2872.
- 3 A. Proust, B. Matt, R. Villanneau, G. Guillemot, P. Gouzerh, G. Izzet, *Chem. Soc. Rev.*, 2012, **41**, 7605.
- 4 (a) C. Y. Duan, M. L. Wei, D. Guo, C. He and Q. J. Meng, *J. Am. Chem. Soc.*, 2010, **132**, 3321; (b) X. Meng, C. Qin, X. L. Wang, Z. M. Su, B. Li and Q. H. Yang, *Dalton Trans.*, 2011, **40**, 9964; (c) A. Iturraspe, B. Artetxe, S. Reinoso, L. S. Felices, P. Vitoria, L. Lezama and J. M. Gutiérrez-Zorrilla, *Inorg. Chem.*, 2013, **52**, 3084; (d) X. L. Wang, Q. Gao, A. X. Tian and G. C. Liu, *Cryst. Growth Des.*, 2012, **12**, 2346.
- 5 (a) Y. Q. Xu, Y. Z. Gao, W. Wei, Z. Q. Wang, S. Li and C. W. Hu, *Dalton Trans.*, 2013, **42**, 5228; (b) P. P. Zhang, J. Peng, H. J. Pang, J. Q. Sha, M. Zhu, D. D. Wang, M. G. Liu and Z. M. Su, *Cryst. Growth Des.*, 2011, **11**, 2736; (c) X. L. Wang, H. L. Hu, A. X. Tian, H. Y. Lin, J. Li, L. M. Shi, *Inorg. Chem. Commun.*, 2010, **13**, 745.
- 6 (a) M. Sarma, T. Chatterjee and S. K. Das, *Inorg. Chem. Commun.*, 2010, **13**, 1114; (b) M. Sarma, T. Chatterjee, H. Vindhya and S. K. Das, *Dalton Trans.*, 2012, **41**, 1862; (c) G. L. Guo, Y. Q. Xu, B. K. Chen, Z. G. Lin and C. W. Hu, *Inorg. Chem. Commun.*, 2011, **14**, 1448.
- 7 (a) R. K. Tan, S. X. Liu, W. Zhang, S. J. Li and Y. Y. Zhang, *Inorg. Chem. Commun.*, 2011, **14**, 384; (b) H. Chen, H. Y. An, X. Liu, H. L. Wang, Z. F. Chen, H. Zhang and Y. Hu, *Inorg. Chem. Commun.*, 2012, **21**, 65; (c) X. L. Wang, Z. H. Chang, H. Y. Lin, A. X. Tian, G. C. Liu and J. W. Zhang, *Dalton Trans.*, 2014, **43**, 12272.
- 8 (a) Y. Hu, F. Luo and F. F. Dong, *Chem. Commun.*, 2011, **47**, 761; (b) Y. L. Teng, B. X. Dong, J. Peng, S. Y. Zhang, L. Chen, L. Song and J. Ge, *CrystEngComm*, 2013, **15**, 2783; (c) X. L. Wang, C. H. Gong, J. W. Zhang, L. L. Hou, J. Luan and G. C. Liu, *CrystEngComm*, 2014, **16**, 7745.
- 9 (a) C. Y. Yang, L. C. Zhang, Z. J. Wang, L. Wang, X. H. Li and Z. M. Zhu, *J. Solid State Chem.*, 2012, **194**, 270; (b) D. Y. Shi, C. He, B. Qi, C. Chen, J. Y. Niu and C. Y. Duan, *Chem. Sci.*, 2015, **6**, 1035; (c) C. J. Zhang, H. J. Pang, Q. Tang and Y. G. Chen, *Dalton Trans.*, 2012, **41**, 9365.
- 10 (a) J. Q. Sha, L. Y. Liang, J. W. Sun, A. X. Tian, P. F. Yan, G. M. Li and C. Wang, *Cryst. Growth Des.*, 2012, **12**, 894; (b) G. F. Hou, L. H. Bi, B. Li, B. Wang and L. X. Wu, *CrystEngComm*, 2011, **13**, 3526; (c) X. L. Wang, J. Li, A. X. Tian, D. Zhao, G. C. Liu and H. Y. Lin, *Cryst. Growth Des.*, 2011, **11**, 3456; (d) Z. K. Qi, J. L. Liu, J. J. Hou, M. M. Liu and X. M. Zhang, *Cryst. Growth Des.*, 2014, **14**, 5773.
- 11 (a) Y. N. Chi, F. Y. Cui, A. R. Jia, X. Y. Ma and C. W. Hu, *CrystEngComm.*, 2012, **14**, 3183; (b) S. B. Li, H. Y. Ma, H. J. Pang and L. Zhang, *Cryst. Growth Des.*, 2014, **14**, 4450.
- 12 (a) J. Niu, J. Hua, X. Ma and J. Wang, *CrystEngComm.*, 2012, **14**, 4060; (b) M. L. Han, X. H. Chang, X. Feng, L. F. Ma and L. Y. Wang, *CrystEngComm.*, 2014, **16**, 1687.
- 13 (a) A. B. Lago, R. Carballo, S. Rodríguez-Hermida and E. M. Vázquez-López, *Cryst. Growth Des.*, 2014, **14**, 3096; (b) G. D. Zou, Z. Z. He, C. B. Tian, L. J. Zhou, M. L. Feng, X. D. Zhang and X. Y. Huang, *Cryst. Growth Des.*, 2014, **14**, 4430.
- 14 (a) S. D. Han, J. P. Zhao, Y. Q. Chen, S. J. Liu, X. H. Miao, T. L. Hu and X. H. Bu, *Cryst. Growth Des.*, 2014, **14**, 2; (b) J. H. Qin, Y. Y. Jia, H. J. Li, B. Zhao, D. Q. Wu, S. Q. Zang, H. W. Hou and Y. T. Fan, *Inorg. Chem.*, 2014, **53**, 685.
- 15 (a) A. PERLOFF, *Inorg. Chem.*, 1970, **9**, 2228; (b) K. Nomiya, T. Takahashi and T. Shirai, *Polyhedron*, 1987, **6**, 213.
- 16 G. M. Sheldrick, *Acta Cryst. A.*, 2008, **64**, 112.
- 17 Y. Gong, T. Wu, P. G. Jiang, J. H. Lin and Y. X. Yang, *Inorg. Chem.*, 2013, **52**, 777.
- 18 I. D. Brown and D. Altermatt, *Acta Crystallogr., Sect. B*, 1985, **41**, 244.
- 19 (a) V. Coué, R. Dessapt, M. Bujoli-Doeuff, M. Evain and S. Jobic, *Inorg. Chem.*, 2007, **46**, 2824; (b) R. Dessapt, M. Collet, V. Coué, M. Bujoli-Doeuff, S. Jobic, C. Lee and M. -H. Whangbo, *Inorg. Chem.*,

- 2009, **48**, 574; (c) Z. F. Chen, H. Y. An, H. Zhang and Y. Hu, *CrystEngComm.*, 2013, **15**, 4711.
- 20 H. X. Yang, S. Y. Gao, J. Lü, B. Xu, J. X. Lin and R. Cao, *Inorg. Chem.*, 2010, **49**, 736.
- 5 21 D. B. Dang, B. An, Y. Bai and J. Y. Niu, *Dalton Trans.*, 2012, **41**, 13856.
- 22 X. L. Wang, X.J. Liu, A. X. Tian, J. Ying, H. Y. Lin, G. C. Liu and Q. Gao, *Dalton Trans.*, 2012, **41**, 9587.
- 23 (a) T. Kurata, A. Uehara, Y. Hayashi and K. Isobe, *Inorg. Chem.*, 2005, **44**, 2524; (b) S. Inami, M. Nishio, Y. Hayashi, K. Isobe, H. Kameda and T. Shimoda, *Eur. J. Inorg. Chem.*, 2009, 5253; (c) Y. Hayashi, *Coord. Chem. Rev.*, 2011, **255**, 2270; (d) M. Nishio, S. Inami, M. Katayama, K. Ozutsumi and Y. Hayashi, *Inorg. Chem.*, 2012, **51**, 784; (e) M. Nishio, S. Inami and Y. Hayashi, *Eur. J. Inorg. Chem.*, 2013, 1876.
- 15 24 L. M. Dai, W. S. You, E. B. Wang, S. X. Wu, Z. M. Su, Q. H. Du, Y. Zhao and Y. Fang, *Cryst. Growth Des.*, 2009, **9**, 2110.
- 25 X. L. Wang, H. Y. Lin, Y. F. Bi, B. K. Chen and G. C. Liu, *J. Solid State Chem.*, 2008, **181**, 556.
- 20 26 R. Dessapt, M. Collet, V. Coué, M. Bujoli-Doeuff, S. Jobic, C. Lee and M.-H. Whangbo, *Inorg. Chem.*, 2009, **48**, 574.
- 27 Q. G. Zhai, X. Y. Wu, S. M. Chen, Z. G. Zhao and C. Z. Lu, *Inorg. Chem.*, 2007, **46**, 5046.
- 28 H. Y. Zhao, J. W. Zhao, B. F. Yang, H. He and G. Y. Yang, *Cryst. Growth Des.*, 2013, **13**, 5171.
- 25 29 (a) H. X. Yang, T. F. Liu, M. N. Cao, H. F. Li, S. Y. Gao and R. Cao, *Chem. Commun.*, 2010, **46**, 2429; (b) X. L. Wang, C. Xu, H. Y. Lin, G. C. Liu, S. Yang, Q. Gao and A. X. Tian, *CrystEngComm.*, 2012, **14**, 5836.
- 30 30 (a) A. Hiskia, A. Mylonas and E. Papaconstantinou, *Chem. Soc. Rev.*, 2001, **30**, 62; (b) A. Dolbecq, P. Mialane, B. Keita and L. Nadjo, *J. Mater. Chem.*, 2012, **22**, 24509; (c) J. W. Sun, M. T. Li, J. Q. Sha, P. F. Yan, C. Wang, S. X. Li and Y. Pan, *CrystEngComm.*, 2013, **15**, 10584.
- 35 31 J. Lü, J. X. Lin, X. L. Zhao and R. Cao, *Chem. Commun.*, 2012, **48**, 669.

# Polyoxometalate-directed assembly of various multinuclear metal–organic complexes with 4-amino-1,2,4-triazole and selective photocatalysis for organic dyes degradation †

Xiu-Li Wang\*, Chun-Hua Gong, Ju-Wen Zhang, Guo-Cheng Liu, Xiao-Min Kan, Na Xu

Five POM-based metal–organic complexes ranging from 0D trinuclear cluster, 1D chain, 2D network, to 3D framework have been successfully prepared at the presence of citric acid or boric acid or not.

